CCD photometry of nearby Seyfert galaxies in the V, I/R bands. II. Photometry results

V.L. Afanasiev, A.N. Burenkov, V.P. Mikhailov, A.I. Shapovalova

Special Astrophysical Observatory of the Russian AS, Nizhnij Arkhyz 357147, Russia

Abstract. Results are presented of CCD photometry of 15 Seyfert galaxies in two colours (V, I or R). The observations have been carried out with the 1 m Zeiss telescope of the SAO RAS. Direct CCD images taken with S/N=5 allowed measuring of the surface brightness up to $(25.0 - 25.5)^m/\square''$ in V, R bands and $(24.0 - 24.5)^m/\square''$ in I band. For the purpose of comparison the aperture photometry of the objects studied earlier by other authors has been performed. Our results are shown to be consistent within 0.1 stellar magnitude with the data of photoelectric photometry.

For all the galaxies surface brightness profiles averaged in azimuth have been obtained. In the frames of the three–component model of a galaxy (nucleus, bulge, disk) the profiles are decomposed into components by the numerical non–linear least squares and interactive methods. The brightness distribution of the star–like nucleus has been represented by a Gaussian, to represent the disk an exponential law has been applied. The brightness distribution of the bulge was simulated by two functions — Gaussian (particular case of the generalized exponential law) and Vaucouleurs law.

For 14 objects a satisfactory agreement of the observed and theoretical brightness profiles has been obtained using gaussian model bulge profile only. The bulge brightness distribution of only one object (Mrk 3) is well represented by the Vaucouleurs law.

From the results of numerical decomposition of the brightness profiles the component parameters, integral stellar magnitudes of the host galaxies, the bulge and disk contribution to the luminosity of host galaxy as well as the ratio of the nucleus luminosity to the integral radiation of the host galaxy have been estimated.

Key words: galaxies: Seyfert – galaxies: CCD photometry – galaxies: kinematics and dynamics

1. Introduction

To understand the origin and evolution of active galactic nuclei, one has to study not only the nuclei themselves but also the galaxies they are located in, i.e. host galaxies. It is of prime importance to know how the activity is related to the structure of a host galaxy and to reveal possible differences between the features of Seyfert and normal galaxies.

Morphological studies of Seyfert galaxies have shown that the overwhelming majority of these objects belong to the class of spiral systems. It was noted by Seyfert (1943) and confirmed later (Adams, 1977; Simkin et al., 1980; MacKenty, 1990; Granato et al., 1993; Moles et al., 1995). This fact by itself may suggest the activity and the structure of the galaxy to be related. In the papers by Simkin et al. (1980) and Su & Simkin (1980) Seyfert galaxies were classified by the degree of concentration of brightness towards the centre, by the presence of inner and outer rings and by the visibility of spiral arms. A correlation of the introduced morphological types with the parameters that characterize the nucleus activity (emission line width, X–ray luminosity) has been found.

Results of the latest morphological investigations allow the conclusion to be drawn that most of the isolated Seyfert galaxies show the presence of non-axisymmetric perturbations of the gravitation potential of type of bars and/or rings (Moles et al., 1995; Márquez, 1996). Some galaxies classified as nonbarred spirals from the optical data reveal a bar in the near IR (McLeod & Rieke, 1994; Mulchaey et al., 1997). The presence of such structures is interpreted as evidence of additional fueling the nucleus with gas.

Besides the morphology studies, in many papers the relationship between the activity and the parameters of distribution of matter in Seyfert galaxies was investigated. A comparison of the volume luminosity of the spheroids of Seyfert and normal galaxies

with the luminosity of their nuclei indicates that the galaxies having more pronounced spheroids and more extended disks possess more active nuclei (Afanasiev, 1987). These results are consistent with the conclusions drawn in the papers by Whittle (1992a, b, c) and Nelson and Whittle (1995, 1996) where the influence of circumnuclear gravitation potential on the formation of properties of active nuclei is studied. The correlation between the orientation of the large–scale bars of Seyfert galaxies and the [OIII] emission line width (Mikhailov, 1986) may also point to the key role of the circumnuclear gravitation potential in the formation of the velocity field in NLR.

A number of authors have come to a conclusion that there is no significant difference in photometric parameters of host Seyfert galaxies and in those of normal galaxies of similar morphological types: for the central surface brightness of the disks (MacKenty, 1990; Granato et al., 1993; etc.) and their characteristic lengths (Yee, 1983; Mediavilla, 1989; MacKenty, 1990; Granato et al., 1993; etc.); for the surface brightness of bulges (Afanasiev et al., 1986; Granato et al., 1993; Mediavilla, 1989, etc.); for colours of disks (Yee, 1983; MacKenty, 1990; Afanasiev et al., 1986); for absolute magnitudes (Afanasiev et al., 1986); for masses (Afanasiev, 1981); etc. Other researchers have revealed these differences: the central surface brightness of the disks in Seyfert galaxies is higher by 1–2 stellar magnitudes (Yee, 1983; Mediavilla, 1989; etc.) and they are "bluer" than those of normal galaxies (Zasov & Lyuty, 1973, 1981; Zasov & Neizvestny, 1989; McLeod & Rieke, 1994; etc.) the degree of brightness concentration to the centre is also higher (Zasov & Lyuty, 1973); the average absolute luminosity of host galaxies is higher than that of normal spiral galaxies and corresponds to that of host galaxies of close quasars (Yee, 1983); mass to luminosity ratio (M/L$\sim$ 5) is essentially lower than that of normal galaxies (M/L$\sim$ 10) (Afanasiev, 1981) and so on.

Thus, the photometric study of Seyfert galaxies yield ambiguous results. This is probably due to both the selection of objects (the principles of sampling are different) and the use of different telescopes and detectors (different photometric limits, spatial resolution, colour bands, etc.). Until recently detailed photometric data would be obtained photographically, which made it difficult to study galaxies with active nuclei because of the great difference in brightness of the nucleus and the host galaxy. That is why photometry data for galaxies with a Seyfert nucleus turned out to be sparse as compared to normal galaxies.

The use of CCDs enable two–dimensional images in a wide dynamic range to be obtained. Over the last few years a great number of CCD photometry data in different colour bands for nearby normal galaxies of different morphological types have appeared (Wozni-

ak et al., 1995; de Jong & van Kruit, 1994; de Jong, 1996). However, for Seyfert galaxies information of such a kind with good limits ($\approx 25 - 26$ $^m/\square''$ in V) is scanty.

So, deep photometry of the Seyfert galaxies for reliable determination of the global photometric parameters of different subsystems (nucleus, bulge, disk) is as before the actual problem of current concern.

We selected for the study Seyfert galaxies of the northern sky (b>0) with z<0.03 and mb<15.7 from the catalogue of Lipovetsky et al. (1987). (The sample comprising 50 objects is complete up to mb=14.5). For nearly all the programme objects FWHM of [OIII] lines are known, for 22 galaxies [OIII] images are available, in 22 galaxies elongated linear radio structures have been detected. Two tens of the objects have no morphological classification. In most galaxies photometric characteristics are not studied. A total of about 70 objects are included in the programme. For the investigation V, I(R) colour bands are chosen, so as to reliably separate both the young and the old population of host galaxies. Besides, in the R(I) bands the influence of dust on the radiation characteristics is reduced.

The main goal of our investigation is to study morphological and photometric characteristics of a homogeneous sample of nearby Seyfert galaxies and to compare them with analogous parameters of normal galaxies of the same morphological types.

In the given paper results are presented of photometry for 15 Seyfert galaxies from our sample. The detailed study of morphology of these objects has been done in the paper by Afanasiev et al. (1998). Comparison of their properties with the characteristics of normal galaxies as well as the results for other objects of the sample will appear in further papers.

2. Observations and reduction

The observations were performed with the 1 m Zeiss telescope of SAO RAS in the V (Johnson) and I/R (Cousins) bands with the 530 × 580 CCD (Afanasiev et al., 1991). The scale was 15.7''/mm, the pixel size was 0''.29 × 0''.38.

The data reduction procedure is reported in detail in the paper by Afanasiev et al. (1998) and involves the following stages: 1) subtraction of electronic bias; 2) flat field correction; 3) removal of cosmic particle traces and correction of values in defective channels; 4) transformation of the scale; 5) sky subtraction.

The bias frame and the flat field image were determined as a median mean from a series of exposures. After the scale transformation the pixel size in the image equals 0''.44. The corrected images were smoothed with a median filter with a window of 3 × 3 pixels. The sky background was subtracted with the

application of bilinear interpolation from image elements after masking the galaxy and field stars. For the purpose of photometric calibration of images, several fields with standard stars were observed on each night (Christian et al., 1985; Landolt, 1992).

Some data on the objects under study are given in Table 1. It should be noted that in most of the galaxies presented in the table bars, inner/outer rings and structures of type "bar within bar" were detected (Afanasiev et al., 1998).

3. Aperture photometry

For individual objects aperture photometry was performed to compare with the data of other authors. For the comparison the photoelectric measurements from the works of Neizvestny (1988) and Doroshenko & Terebizh (1979, 1981), as well as the results of CCD photometry from Kotilainen et al. (1993) were taken. The V, R and I magnitudes in those papers are given in Johnson system. To compare with our results, the data in the R and I bands were converted to the system of Cousins (1976) using the following formulae (de Vaucouleurs & Longo, 1988):
$$(V - R)_C = (V - R)_J/1.428;$$
$$(V - I)_C = (V - I)_J/1.287.$$

The results of the comparison are presented in Table 2 and Fig. 1, where it is seen that for most galaxies our data are in agreement with the results of other researchers within 0.1 stellar magnitude. The considerable differences for the nuclei of individual galaxies (e.g. ≈ 0.3 stellar magnitude for Mrk 533) are due to the variability of their nuclei. According to Neizvestny (1988), the radiation from the nuclei of the galaxies Mrk 3, Mrk 533 and Mrk 573 is variable. On time scales of several months the variability amplitude in the V is 0.22^m, 0.38^m, 0.30^m for Mrk 3, Mrk 533 and Mrk 573, respectively.

In the case of Mrk 3 the surface brightness in the I band is systematically by ≈ 0.4 magnitude lower, while in V it is systematically by ≈ 0.2 stellar magnitude higher as compared to the results of Kotilainen et al. (1993). At the same time, in the V band our data are consistent with the results obtained by Neizvestny (1988) within 0.07 stellar magnitude, excluding a nucleus. It may be assumed that in the I band our measurements have a systematic error of ≈ 0.4 stellar magnitude, whereas in the V band a systematic error of $\approx 0.2^m$ is present in the data of Kotilainen et al. (1993).

4. Decomposition of surface brightness profiles into components

The main goal of the paper is determination of parameters of the spherical and flat subsystems of Seyfert galaxies and evaluation of the share of radiation of

Figure 1: *Comparison of the results of aperture photometry in the V and R bands with the data of other authors. On the abscissa on the diagrams (a, c) the magnitudes taken from the papers of other authors are plotted, on the diagrams (b, d) — aperture in arcseconds. On the ordinate differences of the magnitudes are plotted. The circles are for the data taken from the paper by Neizvestny (1988), the squares are for the data of Doroshenko and Terebizh (1979, 1981), the asterisks mark Kotilainen et al. (1993) data.*

different components (nucleus, bulge, disk) in the integral luminosity of the galaxy. To perform this task, one-dimensional surface brightness profiles were obtained by averaging in an elliptical ring. The parameters of the ellipse were derived from the results of elliptical approximation of isophotes (Afanasiev et al., 1998). The coordinates of the centres of ellipses were determined from the isophotes in the central part of the galaxy. The position angle and the ellipse oblateness were calculated from the outer isophotes in the V band $(25 - 26^m/\square'')$. The results are presented in Table 3 and Fig. 2. The parameters of the ellipses for plotting the profiles are listed in Table 4.

Table 1: *(1, 2) — object name; (3) — Seyfert type; (4) — morphological type according to RC3 catalogue; (5) — additional morphological data from Afanasiev et al. (1998).*

Name (1)	Other (2)	Sy (3)	RC3 type (4)	Revised morphology (5)
Mrk 3	UGC 3426	2.0	S0:	Bar at $r \sim 15''$
Mrk 530	NGC 7603	1.0	SA(rs)b: pec	Possible bar at $r \sim 14''$, ring at $r \sim 20''$
Mrk 533	NGC 7674	2.0	SA(r)bc pec	Bar at $r \sim 8''$;no inner ring
Mrk 573	UGC 1214	2.0	(R)SAB(rs)0+:	Double bar: $r \sim 2.''6$ and $\sim 9''$ inner ring at $r \sim 10''$
Mrk 744	NGC 3786	1.8	SAB(rs)a pec	Double bar: $r \sim 7''$ and $\sim 25''$ outer ring
Mrk 955	MCG 0-2-94	2.0	S?	Bar at $r \sim 15''$; inner and outer rings
Mrk 1058		2.0	S?	Bar at $r \sim 12''$
Mrk 1066	UGC 2456	2.0	(R)SB(s)0+	Double bar: $r \sim 3''$ and $r \sim 15''$;
Mrk 1073	UGC 2608	2.0	(R')SB(s)b	Bar at $r \sim 12''$
Mrk 1157	NGC 591	2.0	(R')SB0	Bar at $r \sim 15''$, inner and outer rings
NGC 1019	UGC 2131	1.0	SB(rs)bc	Pronounced bar at $r \sim 10''$; no inner ring
NGC 3185	UGC 5554	1.0	(R)SB(r)a	Double bar: $r \sim 2.''3$ and $\sim 30''$ no inner ring, outer ring
UGC 524	MCG 5-3-13	1.0	(R')SB(s)b	Bar at $r \sim 9''$; inner and outer rings
UGC 3223	MCG 1-13-12	1.0	SBa	Bar at $r \sim 5''$, inner and outer rings
UGC 3995	MCG 5-19-1	2.0	S pec	Bar at $r \sim 15''$

The surface brightness profiles were analysed on the basis of a three–component model. In the frame of this model the galaxy seems to be composed of a spheroidal (bulge) and a flat (disk) subsystems and a star–like nucleus as well.

The function most frequently used to describe the surface brightness distribution of the disks of spiral galaxies is an exponential law, which in stellar magnitudes can be written as:

$$m_d(r) = m_0 + 1.086r/r_0, \qquad (1)$$

where m_0 is the surface brightness at the centre, r_0 is the scale factor of the disk.

To describe the bulge profile, the functions approximating the profiles of brightness distribution of elliptical galaxies are generally applied. The most extensively used is the Vaucouleurs law ($r^{1/4}$) (de Vaucouleurs, 1948) which can be written in stellar magnitudes as:

$$m_b(r) = m_e + 8.325((r/r_e)^{1/4} - 1), \qquad (2)$$

where m_e is the surface brightness at a distance r_e, r_e is the effective radius (radius of the circle enclosed

half of the bulge luminosity). However, in contrast to the profiles of the disks the model bulge profile shape is not so unquestionable, and there exist a number of other functions proposed by different authors, for instance the Hubble profile (Hubble, 1930), the King profile (King, 1966), the generalized exponential law (Caon et al., 1993; D'Onofrio et al., 1994) (see for details the paper by de Jong (1996) and references therein). One of the most common ways to describe the bulge profile is the generalized exponential law:

$$I(r) = I_0 e^{-(r/r_0)^{1/n}}. \qquad (3)$$

When setting $n = 4$ and redetermining the parameters I_0 and r_0, (3) is transformed to form (2). In the case $n = 0.5$ (3) is converted to a Gauss function, which in stellar magnitudes can be written as:

$$m_b(r) = m_0 + 0.543r^2/\sigma^2, \qquad (4)$$

where m_0 is the surface brightness at the centre, σ is the Gaussian scale parameter. Having determined the parameters of function (4), we can estimate the radius of the circle enclosed half of the bulge luminosity ($r_e = 0.683\sigma$), and the surface brightness at that

Table 2: *Comparison with aperture photometry of other authors*

Object (1)	Band (2)	A (3)	SAO (4)	Data (5)	Other (6)	Data (7)	Ref. (8)	Δm (9)
Mrk3	V	4.3	14.32	06.12.94	14.21	16.10.83	a	0.11
	V	13.8	13.42		13.47	24.01.79	a	-0.05
	V	13.8	13.42		13.41	11.11.83	a	0.01
	V	13.8	13.42		13.49	28.10.83	a	-0.05
	V	17.2	13.31		13.39	16.10.83	a	-0.08
	V	28.9	13.05		13.15	11.11.82	a	-0.10
	V	37.5	12.94		13.03	11.11.82	a	-0.09
	V	55.0	12.80		12.86	03.03.81	a	-0.06
	V	55.0	12.80		12.90	11.11.82	a	-0.10
	V	75.6	12.73		12.79	24.01.79	a	-0.06
	V	75.6	12.73		12.76	11.11.82	a	-0.03
Mrk530	V	13.8	14.00	07.12.94	14.15	15.08.80	a	-0.15
	V	28.9	13.55		13.63		a	-0.08
	V	37.5	13.39		13.45		a	-0.06
	V	55.0	13.19		13.27		a	-0.08
	V	75.6	13.09		13.04		a	0.05
Mrk533	V	6.9	15.23	04.09.94	14.92	27.07.84	a	0.31
	V	13.8	14.63		14.58	25.09.81	a	0.05
	V	17.2	14.39		14.35	27.07.84	a	0.04
	V	28.9	13.85		13.87	25.09.81	a	-0.02
	V	37.5	13.63		13.68	25.09.81	a	-0.05
	V	55.0	13.33		13.32		a	0.01
	V	75.6	13.09		13.03	29.07.81	a	0.06
	V	75.6	13.09		12.98	25.09.81	a	0.11
Mrk 573	V	3.0	15.51	04.09.94	15.51	26.12.92	d	0.00
	V	6.0	14.71		14.74		d	-0.03
	V	6.9	14.59		14.67	21.10.84	a	-0.08
	V	9.0	14.39		14.42		a	-0.03
	V	9.0	14.39		14.42	26.12.92	d	-0.03
	V	11.7	14.22		14.13	21.10.84	a	0.09
	V	12.0	14.21		14.21	26.12.92	d	0.00
	V	13.8	14.12		14.11	08.09.80	a	0.01
	V	13.8	14.12		14.06	25.09.81	a	0.06
	V	17.2	13.98		13.97	21.10.84	a	0.01
	V	23.6	13.80		13.69		a	0.11
	V	28.9	13.73		13.62	08.09.80	a	0.11
	V	37.5	13.66		13.52	08.09.80	a	0.14
Mrk744	V	25.0	13.83	09.02.94	13.74	28.02.79	b	0.09
	V	25.0	13.83		13.74	18.03.79	b	0.09
	V	28.9	13.68		13.69	11.03.80	a	-0.01
	V	28.9	13.68		13.66	01.03.81	a	0.02
	V	37.5	13.39		13.32	11.03.80	a	0.07
	V	37.5	13.39		13.34	01.03.81	a	0.05
	V	55.0	13.06		13.04		a	0.02
	V	55.0	13.06		12.94	18.03.79	b	0.12
	V	75.6	12.88		12.71	10.03.81	a	0.17
Mrk955	V	28.9	14.42	05.09.94	14.09	01.10.84	a	0.33
	V	55.0	14.20		14.01		a	0.19
Mrk1058	V	28.9	14.63	05.09.94	14.72	18.08.82	a	-0.09
	V	28.9	14.63		14.54	01.10.84	a	0.09
	V	55.0	14.40		14.38	18.08.82	a	0.02
	V	55.0	14.40		14.31	01.10.84	a	0.09
Mrk1066	V	25.0	14.00	03.09.94	13.96	27.11.79	b	0.04

Table 2: *Comparison with aperture photometry of other authors (continue)*

Object (1)	Band (2)	A (3)	SAO (4)	Data (5)	Other (6)	Data (7)	Ref. (8)	Δm (9)
	V	25.0	14.00		14.01	18.01.80	c	-0.01
	V	25.0	14.00		14.01		c	-0.01
	V	28.9	13.90		13.92	18.02.82	a	-0.02
	V	37.5	13.75		13.69		a	0.06
	V	55.0	13.60		13.42		a	0.18
	V	75.6	13.42		13.27		a	0.15
Mrk1073	V	25.0	14.12	06.12.94	14.19	27.11.79	b	-0.07
	V	25.0	14.12		14.15	18.12.79	c	-0.03
	V	25.0	14.12		14.18	18.01.80	c	-0.06
	V	28.9	14.00		13.95	01.10.84	a	0.05
	V	55.0	13.62		13.56		a	0.06
Mrk1157	V	28.9	13.79	10.12.94	13.90	02.10.84	a	-0.11
	V	55.0	13.37		13.38		a	-0.01
	V	75.6	13.28		13.20		a	0.08
Mrk533	R	6.9	14.63	22.07.93	14.43	27.07.84	a	0.20
	R	13.8	13.99		13.98	25.09.81	a	0.01
	R	17.2	13.74		13.78	27.07.84	a	-0.04
	R	28.9	13.21		13.31	25.09.81	a	-0.10
	R	37.5	12.99		13.11		a	-0.12
	R	55.0	12.69		12.76		a	-0.07
	R	75.6	12.45		12.48	29.07.81	a	-0.03
	R	75.6	12.45		12.44	25.09.81	a	0.01
Mrk744	R	25.0	13.21	09.02.94	13.11	18.03.79	b	0.10
	R	28.9	13.07		13.10	11.03.80	a	-0.03
	R	28.9	13.07		13.09	01.03.81	a	-0.02
	R	37.5	12.80		12.75	11.03.80	a	0.05
	R	37.5	12.80		12.76	01.03.81	a	0.04
	R	55.0	12.48		12.39	18.03.79	b	0.09
	R	55.0	12.49		12.47	01.03.81	a	0.02
	R	75.6	12.31		12.10		a	0.11
Mrk3	V	3.0	14.75	06.12.94	14.80	25.12.92	d	-0.05
	V	6.0	14.00		14.19		d	-0.19
	V	9.0	13.69		13.90		d	-0.21
	V	12.0	13.51		13.72		d	-0.21
Mrk573	V	3.0	15.51	04.09.94	15.51	26.12.92	d	0.00
	V	6.0	14.71		14.74		d	-0.03
	V	9.0	14.39		14.42		d	-0.03
	V	12.0	14.21		14.21		d	0.00
Mrk3	I	3.0	14.57	06.12.94	13.78	25.12.92	d	0.79
	I	6.0	13.55		13.06		d	0.49
	I	9.0	13.13		12.72		d	0.41
	I	12.0	12.89		12.50		d	0.39
Mrk573	I	3.0	14.48	04.09.94	14.47	26.12.92	d	0.01
	I	6.0	13.68		13.72		d	-0.03
	I	9.0	13.36		13.39		d	-0.03
	I	12.0	13.16		13.19		d	-0.03

Notes: (1) - the object name; (2) - filter; (3) - aperture in arcseconds; (4) - stellar magnitude in a given aperture (our measurements); (5) - date of the observation; (6) - stellar magnitude in a given aperture (other authors' data); (7) - date of the observations; (8) - references: (a) - Neizvestny, 1988; (b) - Doroshenko, Terebizh, 1979; (c) - Doroshenko, Terebizh, 1981; (d) - Kotilainen et al., 1993; (9) - difference in data between our and other authors' results.

Table 3: *Observed surface brightness profiles*

| r | Mrk 3 | | Mrk 530 | | Mrk 533 | | Mrk 573 | | Mrk 744 | | Mrk 955 | | Mrk 1058 | | Mrk 1066 | |
(")	I	V	I	V	R	V	I	V	R	V	I	V	I	V	I	V
0.0	16.4	16.4	15.8	16.5	17.4	17.4	16.2	17.1	17.3	18.0	17.2	18.1	17.2	18.5	16.4	17.8
0.5	16.5	16.5	16.0	16.8	17.6	17.7	16.3	17.3	17.4	18.1	17.3	18.2	17.3	18.6	16.5	17.9
1.0	16.6	16.8	16.3	17.0	17.9	18.1	16.6	17.7	17.4	18.2	17.4	18.4	17.5	18.8	16.7	18.0
1.5	16.9	17.3	16.7	17.5	18.4	18.7	17.0	18.0	17.6	18.3	17.7	18.7	17.7	19.0	16.8	18.3
2.0	17.2	17.7	17.1	18.0	18.8	19.2	17.4	18.5	17.8	18.5	18.0	19.1	17.9	19.3	17.1	18.5
2.5	17.4	18.2	17.5	18.5	19.2	19.7	17.8	18.8	18.1	18.7	18.3	19.4	18.2	19.6	17.4	18.8
3.0	17.7	18.5	17.8	18.9	19.5	20.0	18.2	19.2	18.3	19.0	18.6	19.8	18.4	19.8	17.7	19.1
3.5	18.0	18.8	18.1	19.1	19.7	20.2	18.5	19.5	18.5	19.2	18.9	20.1	18.7	20.1	18.0	19.4
4.0	18.2	19.1	18.3	19.4	19.9	20.4	18.8	19.8	18.8	19.4	19.2	20.4	18.9	20.3	18.2	19.7
4.5	18.5	19.3	18.5	19.6	20.0	20.5	19.0	20.1	19.0	19.6	19.4	20.7	19.1	20.5	18.5	19.9
5.0	18.7	19.5	18.7	19.8	20.2	20.6	19.2	20.3	19.1	19.8	19.7	20.9	19.3	20.6	18.7	20.1
5.5	18.8	19.7	18.8	20.0	20.2	20.7	19.4	20.5	19.3	19.9	19.9	21.1	19.4	20.8	18.9	20.3
6.0	19.0	19.9	19.0	20.1	20.3	20.8	19.6	20.7	19.4	20.1	20.1	21.3	19.6	21.0	19.1	20.5
6.5	19.2	20.1	19.1	20.3	20.4	20.8	19.7	20.8	19.6	20.2	20.3	21.5	19.7	21.1	19.2	20.6
7.0	19.3	20.2	19.2	20.4	20.4	20.9	19.8	20.9	19.7	20.3	20.4	21.7	19.9	21.2	19.4	20.7
7.5	19.5	20.4	19.4	20.5	20.5	20.9	19.9	21.0	19.8	20.4	20.6	21.8	20.0	21.3	19.5	20.8
8.0	19.6	20.5	19.5	20.7	20.5	20.9	19.9	21.1	19.9	20.5	20.7	21.9	20.1	21.5	19.6	20.9
8.5	19.7	20.6	19.6	20.8	20.6	21.0	20.0	21.2	20.0	20.6	20.8	22.0	20.2	21.6	19.7	21.0
9.0	19.8	20.8	19.7	20.9	20.6	21.0	20.1	21.2	20.0	20.6	21.0	22.1	20.3	21.6	19.8	21.1
9.5	19.9	20.9	19.8	21.0	20.7	21.1	20.2	21.3	20.1	20.7	21.1	22.2	20.4	21.7	19.9	21.2
10.0	20.1	21.0	19.9	21.0	20.8	21.2	20.3	21.4	20.2	20.8	21.2	22.2	20.5	21.8	20.0	21.3
10.5	20.2	21.1	20.0	21.1	20.8	21.3	20.4	21.6	20.2	20.8	21.2	22.3	20.5	21.9	20.1	21.4
11.0	20.3	21.2	20.0	21.1	20.9	21.3	20.6	21.7	20.3	20.9	21.3	22.4	20.6	21.9	20.2	21.5
11.5	20.4	21.2	20.1	21.2	21.0	21.4	20.8	21.9	20.3	20.9	21.4	22.4	20.7	22.0	20.3	21.5
12.0	20.5	21.3	20.2	21.3	21.1	21.5	21.0	22.0	20.4	20.9	21.5	22.5	20.8	22.1	20.3	21.6
12.5	20.6	21.4	20.3	21.3	21.1	21.5	21.2	22.2	20.4	21.0	21.5	22.6	20.9	22.1	20.4	21.7
13.0	20.7	21.5	20.3	21.4	21.2	21.6	21.3	22.3	20.5	21.0	21.6	22.6	21.0	22.2	20.5	21.7
13.5	20.8	21.5	20.4	21.4	21.3	21.7	21.6	22.5	20.5	21.1	21.7	22.7	21.0	22.3	20.5	21.8
14.0	20.8	21.6	20.5	21.5	21.4	21.7	21.8	22.7	20.5	21.1	21.7	22.7	21.1	22.3	20.6	21.8
14.5	20.9	21.7	20.5	21.5	21.4	21.8	22.0	22.8	20.6	21.1	21.8	22.8	21.2	22.4	20.7	21.9
15.0	21.0	21.7	20.6	21.6	21.5	21.9	22.2	22.9	20.6	21.2	21.9	22.9	21.3	22.5	20.7	22.0
15.5	21.1	21.8	20.7	21.6	21.6	21.9	22.6	23.0	20.6	21.2	22.0	22.9	21.3	22.6	20.8	22.0
16.0	21.2	21.9	20.7	21.7	21.6	22.0	22.6	23.2	20.7	21.2	22.1	23.0	21.4	22.6	20.8	22.0
16.5	21.3	21.9	20.8	21.7	21.7	22.1	22.8	23.3	20.7	21.2	22.2	23.1	21.5	22.7	20.9	22.1
17.0	21.4	22.0	20.8	21.7	21.7	22.1	22.9	23.3	20.7	21.3	22.4	23.2	21.6	22.8	21.0	22.1
17.5	21.4	22.1	20.9	21.8	21.8	22.2	23.0	23.4	20.7	21.3	22.5	23.3	21.7	22.9	21.0	22.2
18.0	21.5	22.1	20.9	21.8	21.8	22.2	23.1	23.5	20.7	21.3	22.6	23.5	21.7	22.9	21.1	22.3
18.5	21.6	22.2	21.0	21.9	21.9	22.3	23.1	23.6	20.7	21.3	22.7	23.6	21.8	23.0	21.2	22.3
19.0	21.7	22.3	21.0	21.9	22.0	22.3	23.1	23.6	20.8	21.3	22.9	23.7	21.9	23.1	21.3	22.4
19.5	21.8	22.3	21.1	22.0	22.0	22.4	23.2	23.6	20.8	21.3	23.0	23.8	22.0	23.2	21.3	22.5
20.0	21.9	22.4	21.2	22.0	22.0	22.4	23.2	23.6	20.8	21.4	23.2	23.9	22.1	23.3	21.4	22.6
20.5	21.9	22.4	21.2	22.1	22.1	22.4	23.2	23.6	20.8	21.4	23.3	24.1	22.2	23.4	21.5	22.6
21.0	22.0	22.5	21.3	22.1	22.1	22.5	23.3	23.6	20.8	21.4	23.4	24.1	22.4	23.5	21.6	22.7
21.5	22.1	22.6	21.3	22.1	22.2	22.5	23.3	23.7	20.9	21.4	23.5	24.2	22.5	23.6	21.7	22.8
22.0	22.1	22.6	21.4	22.2	22.2	22.6	23.2	23.6	20.9	21.4	23.6	24.3	22.6	23.8	21.8	22.9
22.5	22.2	22.7	21.4	22.2	22.3	22.6	23.2	23.7	20.9	21.5	23.7	24.3	22.7	23.9	21.9	23.0
23.0	22.3	22.8	21.5	22.3	22.3	22.7	23.3	23.7	21.0	21.5	23.7	24.4	22.9	24.0	22.0	23.0
23.5	22.4	22.8	21.5	22.3	22.4	22.7	23.3	23.7	21.0	21.5	23.8	24.5	23.0	24.1	22.1	23.1
24.0	22.5	22.9	21.6	22.4	22.5	22.8	23.3	23.8	21.0	21.6	23.8	24.5	23.1	24.2	22.2	23.2
24.5	22.5	22.9	21.7	22.4	22.5	22.8	23.4	23.8	21.1	21.6	23.8	24.5	23.3	24.3	22.2	23.3
25.0	22.6	23.0	21.7	22.5	22.6	22.9	23.4	23.8	21.1	21.7	23.9	24.6	23.4	24.4	22.4	23.4
25.5	22.7	23.1	21.8	22.5	22.6	22.9	23.4	23.9	21.2	21.7	–	24.6	23.6	24.6	22.5	23.5
26.0	22.8	23.1	21.8	22.5	22.7	23.0	23.5	23.9	21.2	21.8	–	24.6	23.7	24.7	22.6	23.6
26.5	22.9	23.2	21.9	22.6	22.8	23.0	23.6	24.0	21.3	21.8	–	24.7	23.8	24.8	22.7	23.7
27.0	23.0	23.2	21.9	22.6	22.8	23.1	23.6	24.0	21.3	21.8	–	24.7	24.0	24.9	22.8	23.7
27.5	23.0	23.3	22.0	22.7	22.9	23.1	23.7	24.1	21.4	21.9	–	24.8	24.1	25.0	22.8	23.9
28.0	23.1	23.4	22.0	22.7	22.9	23.2	23.7	24.1	21.4	22.0	–	24.8	24.1	25.0	22.9	23.9
28.5	23.1	23.4	22.1	22.8	23.0	23.2	23.8	24.1	21.5	22.0	–	24.8	24.1	25.1	23.0	24.0
29.0	23.3	23.5	22.1	22.8	23.0	23.2	23.8	24.2	21.5	22.1	–	24.9	24.2	25.2	23.0	24.0
29.5	23.3	23.5	22.2	22.8	23.1	23.3	23.8	24.3	21.6	22.1	–	24.9	24.3	25.4	23.1	24.1

Table 3: *Observed surface brightness profiles (continue)*

r ('')	Mrk 3 I	Mrk 3 V	Mrk 530 I	Mrk 530 V	Mrk 533 R	Mrk 533 V	Mrk 573 I	Mrk 573 V	Mrk 744 R	Mrk 744 V	Mrk 955 I	Mrk 955 V	Mrk 1058 I	Mrk 1058 V	Mrk 1066 I	Mrk 1066 V
30.0	23.4	23.6	22.3	22.9	23.2	23.4	23.8	24.3	21.6	22.2	–	25.0	24.5	25.5	23.2	24.1
30.5	23.4	23.6	22.3	23.0	23.3	23.4	–	24.4	21.7	22.2	–	25.0	–	–	23.2	24.2
31.0	23.5	23.7	22.4	23.0	23.4	23.5	–	24.4	21.7	22.2	–	25.0	–	–	23.3	24.2
31.5	23.6	23.7	22.4	23.0	23.5	23.6	–	24.4	21.8	22.3	–	25.1	–	–	23.3	24.3
32.0	23.7	23.8	22.5	23.1	23.6	23.7	–	24.5	21.8	22.3	–	25.1	–	–	23.3	24.3
32.5	23.7	23.8	22.5	23.1	23.7	23.8	–	24.6	21.9	22.4	–	25.2	–	–	23.4	24.4
33.0	23.8	23.9	22.6	23.2	23.7	23.8	–	24.7	21.9	22.4	–	25.2	–	–	23.4	24.4
33.5	23.8	23.9	22.7	23.2	23.9	23.9	–	24.7	22.0	22.5	–	25.3	–	–	23.4	24.4
34.0	23.8	24.0	22.7	23.3	24.0	24.0	–	24.8	22.0	22.5	–	25.4	–	–	23.5	24.5
34.5	23.9	24.0	22.8	23.3	24.1	24.1	–	24.8	22.1	22.6	–	25.4	–	–	23.5	24.5
35.0	23.9	24.1	22.8	23.4	24.2	24.1	–	24.8	22.1	22.6	–	25.4	–	–	23.5	24.5
35.5	22.8	24.1	22.8	23.4	24.4	24.3	–	24.9	22.1	22.6	–	–	–	–	23.6	24.5
36.0	22.9	24.2	22.9	23.5	24.5	24.4	–	24.9	22.2	22.7	–	–	–	–	23.6	24.5
36.5	22.9	24.2	22.9	23.5	24.6	24.5	–	24.9	22.2	22.7	–	–	–	–	23.7	24.6
37.0	23.0	24.2	23.0	23.5	24.7	24.5	–	25.0	22.2	22.7	–	–	–	–	23.7	24.6
37.5	23.1	24.3	23.1	23.6	24.8	24.6	–	25.1	22.2	22.8	–	–	–	–	23.7	24.6
38.0	23.1	24.4	23.1	23.6	24.9	24.6	–	25.1	22.3	22.8	–	–	–	–	23.7	24.6
38.5	23.2	24.4	23.2	23.7	25.0	24.7	–	25.1	22.3	22.8	–	–	–	–	23.7	24.7
39.0	23.2	24.4	23.2	23.7	25.1	24.7	–	25.2	22.3	22.8	–	–	–	–	23.8	24.6
39.5	23.3	24.5	23.3	23.8	25.2	24.8	–	25.3	22.4	22.9	–	–	–	–	23.8	24.6
40.0	23.3	24.5	23.3	23.9	25.2	24.9	–	25.4	22.4	22.9	–	–	–	–	23.8	24.7
40.5	23.5	24.6	23.5	23.9	–	–	–	25.4	22.4	22.9	–	–	–	–	23.8	24.7
41.0	23.5	24.7	23.5	24.0	–	–	–	25.4	22.4	23.0	–	–	–	–	23.8	24.8
41.5	23.6	24.7	23.6	24.0	–	–	–	25.4	22.5	23.0	–	–	–	–	23.8	24.8
42.0	23.7	24.7	23.7	24.1	–	–	–	25.4	22.5	23.0	–	–	–	–	23.9	24.9
42.5	23.8	24.8	23.8	24.2	–	–	–	25.5	22.5	23.0	–	–	–	–	23.9	24.9
43.0	23.9	24.8	23.9	24.2	–	–	–	25.5	22.6	23.1	–	–	–	–	23.9	24.9
43.5	24.0	24.9	24.0	24.2	–	–	–	25.6	22.6	23.1	–	–	–	–	24.0	24.9
44.0	24.0	24.9	24.0	24.3	–	–	–	25.6	22.6	23.1	–	–	–	–	24.0	24.9
44.5	24.1	25.0	24.1	24.4	–	–	–	25.6	22.6	23.1	–	–	–	–	24.1	25.0
45.0	24.1	25.0	24.1	24.4	–	–	–	25.6	22.7	23.2	–	–	–	–	24.1	25.1
45.5	–	–	–	24.5	–	–	–	–	22.7	23.2	–	–	–	–	24.1	25.2
46.0	–	–	–	24.5	–	–	–	–	22.7	23.2	–	–	–	–	24.2	25.2
46.5	–	–	–	24.6	–	–	–	–	22.7	23.2	–	–	–	–	24.3	25.2
47.0	–	–	–	24.7	–	–	–	–	22.8	23.3	–	–	–	–	24.3	25.3
47.5	–	–	–	24.7	–	–	–	–	22.8	23.3	–	–	–	–	24.4	25.4
48.0	–	–	–	24.7	–	–	–	–	22.8	23.3	–	–	–	–	24.5	25.6
48.5	–	–	–	24.8	–	–	–	–	22.8	23.3	–	–	–	–	24.5	25.6
49.0	–	–	–	24.8	–	–	–	–	22.8	23.3	–	–	–	–	24.5	25.6
49.5	–	–	–	24.9	–	–	–	–	22.9	23.4	–	–	–	–	24.6	25.6
50.0	–	–	–	24.9	–	–	–	–	22.9	23.4	–	–	–	–	24.7	25.5
50.5	–	–	–	24.9	–	–	–	–	22.9	23.4	–	–	–	–	–	–
51.0	–	–	–	24.9	–	–	–	–	22.9	23.4	–	–	–	–	–	–
51.5	–	–	–	25.0	–	–	–	–	23.0	23.5	–	–	–	–	–	–
52.0	–	–	–	25.0	–	–	–	–	23.0	23.5	–	–	–	–	–	–
52.5	–	–	–	25.1	–	–	–	–	23.0	23.6	–	–	–	–	–	–
53.0	–	–	–	25.2	–	–	–	–	23.1	23.6	–	–	–	–	–	–
53.5	–	–	–	25.3	–	–	–	–	23.1	23.6	–	–	–	–	–	–
54.0	–	–	–	25.3	–	–	–	–	–	–	–	–	–	–	–	–

Table 3: *Observed surface brightness profiles (continue)*

r	Mrk 1073		Mrk 1157		NGC 1019		NGC 3185		UGC 524		UGC 3223		UGC 3995	
(″)	I	V	I	V	R	V	I	V	I	V	I	V	I	V
0.0	16.7	17.8	16.8	17.8	18.6	19.4	16.9	18.1	16.7	18.0	18.4	18.7	16.8	18.3
0.5	16.9	18.0	17.0	18.0	18.8	19.6	17.0	18.2	16.9	18.2	18.5	18.8	16.9	18.4
1.0	17.1	18.3	17.3	18.3	18.9	19.7	17.1	18.3	17.2	18.4	18.6	18.9	17.0	18.5
1.5	17.5	18.7	17.6	18.8	19.1	19.9	17.3	18.5	17.7	18.9	18.7	19.1	17.2	18.6
2.0	17.8	19.1	18.0	19.2	19.4	20.1	17.5	18.7	18.2	19.3	18.8	19.3	17.3	18.7
2.5	18.2	19.5	18.3	19.5	19.7	20.4	17.7	19.0	18.6	19.8	18.9	19.5	17.6	18.9
3.0	18.4	19.7	18.5	19.7	20.0	20.6	18.0	19.2	19.0	20.2	19.1	19.7	17.8	19.1
3.5	18.6	19.9	18.7	19.9	20.3	20.9	18.2	19.5	19.3	20.5	19.2	19.9	17.9	19.2
4.0	18.8	20.0	18.9	20.1	20.5	21.1	18.4	19.7	19.6	20.7	19.4	20.0	18.2	19.4
4.5	18.9	20.1	19.1	20.2	20.7	21.4	18.6	19.9	19.8	20.9	19.5	20.1	18.3	19.6
5.0	19.0	20.2	19.2	20.4	20.9	21.5	18.8	20.1	20.0	21.1	19.6	20.2	18.5	19.7
5.5	19.1	20.3	19.4	20.5	21.1	21.7	19.0	20.2	20.2	21.3	19.7	20.3	18.6	19.9
6.0	19.2	20.4	19.5	20.6	21.2	21.8	19.1	20.3	20.3	21.4	19.9	20.4	18.7	20.0
6.5	19.3	20.6	19.6	20.7	21.3	21.9	19.2	20.4	20.4	21.5	20.0	20.5	18.9	20.1
7.0	19.5	20.7	19.7	20.8	21.4	22.0	19.3	20.5	20.5	21.6	20.1	20.6	19.0	20.2
7.5	19.6	20.8	19.9	20.9	21.5	22.1	19.4	20.6	20.6	21.7	20.2	20.7	19.1	20.3
8.0	19.7	20.9	20.0	21.0	21.6	22.2	19.5	20.7	20.8	21.8	20.3	20.8	19.2	20.4
8.5	19.8	21.0	20.0	21.0	21.7	22.3	19.5	20.8	20.9	21.9	20.4	20.9	19.3	20.5
9.0	19.9	21.0	20.1	21.1	21.7	22.4	19.6	20.8	21.0	22.0	20.5	21.0	19.4	20.6
9.5	19.9	21.1	20.2	21.2	21.8	22.4	19.7	20.9	21.2	22.1	20.6	21.1	19.5	20.7
10.0	20.0	21.2	20.3	21.2	21.9	22.5	19.8	20.9	21.4	22.3	20.6	21.1	19.5	20.8
10.5	20.1	21.3	20.4	21.3	21.9	22.5	19.8	21.0	21.5	22.4	20.7	21.2	19.6	20.8
11.0	20.2	21.4	20.5	21.4	22.0	22.6	19.9	21.0	21.6	22.5	20.8	21.2	19.7	20.9
11.5	20.3	21.4	20.5	21.5	22.1	22.7	19.9	21.1	21.7	22.6	20.8	21.3	19.8	21.0
12.0	20.4	21.5	20.6	21.6	22.1	22.8	20.0	21.1	21.8	22.6	20.9	21.3	19.8	21.0
12.5	20.5	21.6	20.7	21.6	22.2	22.8	20.0	21.2	21.9	22.7	20.9	21.3	19.9	21.1
13.0	20.6	21.7	20.8	21.7	22.3	22.9	20.1	21.2	21.9	22.8	21.0	21.4	19.9	21.1
13.5	20.7	21.8	20.9	21.8	22.3	22.9	20.1	21.3	21.9	22.8	21.1	21.4	20.0	21.2
14.0	20.8	21.9	21.0	21.9	22.4	23.0	20.2	21.3	22.0	22.8	21.2	21.5	20.0	21.2
14.5	21.0	22.0	21.1	21.9	22.4	23.0	20.2	21.4	22.0	22.8	21.2	21.5	20.1	21.3
15.0	21.1	22.1	21.2	22.0	22.5	23.1	20.3	21.4	22.0	22.8	21.3	21.6	20.1	21.3
15.5	21.1	22.2	21.3	22.1	22.5	23.1	20.4	21.5	22.0	22.8	21.4	21.6	20.2	21.3
16.0	21.2	22.3	21.4	22.2	22.5	23.1	20.4	21.5	22.0	22.8	21.4	21.7	20.2	21.4
16.5	21.3	22.3	21.4	22.2	22.5	23.1	20.5	21.6	22.0	22.8	21.5	21.7	20.2	21.4
17.0	21.4	22.4	21.5	22.3	22.5	23.2	20.5	21.6	22.0	22.8	21.6	21.8	20.3	21.4
17.5	21.4	22.4	21.6	22.4	22.5	23.2	20.5	21.7	22.0	22.7	21.6	21.9	20.3	21.4
18.0	21.4	22.4	21.7	22.5	22.5	23.1	20.6	21.7	22.0	22.7	21.7	21.9	20.3	21.5
18.5	21.5	22.4	21.8	22.6	22.5	23.1	20.6	21.7	21.9	22.6	21.8	22.0	20.4	21.5
19.0	21.5	22.5	21.9	22.6	22.5	23.1	20.6	21.7	21.9	22.6	21.9	22.0	20.4	21.5
19.5	21.6	22.5	21.9	22.7	22.5	23.1	20.7	21.8	21.9	22.6	22.0	22.1	20.4	21.6
20.0	21.6	22.5	22.0	22.7	22.4	23.1	20.7	21.8	21.9	22.6	22.1	22.2	20.5	21.6
20.5	21.6	22.6	22.0	22.8	22.5	23.1	20.7	21.8	21.9	22.6	22.2	22.2	20.5	21.6
21.0	21.7	22.6	22.1	22.8	22.5	23.1	20.8	21.9	21.9	22.6	22.3	22.2	20.6	21.7
21.5	21.8	22.7	22.2	22.9	22.5	23.1	20.8	21.9	21.9	22.6	22.3	22.3	20.6	21.7
22.0	21.8	22.7	22.3	22.9	22.5	23.1	20.8	21.9	21.9	22.6	22.4	22.3	20.7	21.8
22.5	21.9	22.8	22.3	23.0	22.5	23.2	20.8	21.9	21.9	22.7	22.4	22.4	20.7	21.8
23.0	22.0	22.9	22.3	23.0	22.6	23.2	20.8	21.9	22.0	22.7	22.5	22.4	20.8	21.9
23.5	22.0	22.9	22.3	23.0	22.6	23.3	20.9	21.9	22.1	22.8	22.6	22.5	20.9	21.9
24.0	22.1	22.9	22.4	23.0	22.7	23.3	20.9	22.0	22.1	22.8	22.7	22.5	20.9	22.0
24.5	22.1	23.0	22.4	23.0	22.8	23.4	20.9	22.0	22.2	22.9	22.7	22.6	21.0	22.1
25.0	22.2	23.1	22.5	23.1	22.8	23.5	20.9	22.0	22.3	23.0	22.9	22.6	21.0	22.1
25.5	22.2	23.1	22.5	23.1	22.9	23.6	20.9	22.0	22.4	23.1	22.9	22.7	21.1	22.2
26.0	22.3	23.2	22.6	23.1	23.0	23.6	20.9	22.0	22.5	23.2	23.0	22.7	21.1	22.2
26.5	22.4	23.2	22.7	23.2	23.1	23.7	20.9	22.0	22.6	23.3	23.0	22.7	21.1	22.2
27.0	22.5	23.3	22.7	23.2	23.2	23.8	21.0	22.0	22.6	23.4	23.0	22.8	21.2	22.3
27.5	22.6	23.4	22.8	23.3	23.3	23.9	21.0	22.1	22.7	23.4	23.1	22.8	21.2	22.3
28.0	22.7	23.5	23.0	23.4	23.4	24.0	21.0	22.1	22.8	23.5	23.2	22.8	21.2	22.4
28.5	22.8	23.6	23.1	23.5	23.5	24.1	21.0	22.1	22.9	23.6	23.3	22.9	21.3	22.4
29.0	22.8	23.7	23.2	23.6	23.6	24.2	21.0	22.1	23.0	23.7	23.3	22.9	21.3	22.4
29.5	22.9	23.7	23.4	23.7	23.7	24.3	21.0	22.1	23.1	23.8	23.4	23.0	21.4	22.4

Table 3: *Observed surface brightness profiles (continue)*

r (")	Mrk 1073 I	Mrk 1073 V	Mrk 1157 I	Mrk 1157 V	NGC 1019 R	NGC 1019 V	NGC 3185 I	NGC 3185 V	UGC 524 I	UGC 524 V	UGC 3223 I	UGC 3223 V	UGC 3995 I	UGC 3995 V
30.0	23.0	23.8	23.6	23.9	23.8	24.4	21.0	22.1	23.2	23.9	23.4	23.0	21.4	22.4
30.5	23.1	23.9	23.8	24.0	23.8	24.5	21.0	22.1	23.3	24.0	23.5	23.0	21.4	22.5
31.0	23.2	24.0	24.0	24.1	23.9	24.6	21.0	22.1	23.4	24.1	23.5	23.0	21.4	22.5
31.5	23.4	24.1	24.2	24.3	24.0	24.6	21.0	22.1	23.4	24.2	23.6	23.1	21.4	22.5
32.0	23.5	24.2	24.2	24.4	24.0	24.7	21.0	22.1	23.5	24.3	23.6	23.1	21.4	22.5
32.5	23.7	24.3	24.3	24.6	24.1	24.7	21.1	22.1	23.6	24.4	23.7	23.2	21.5	22.5
33.0	23.7	24.4	24.3	24.6	24.2	24.8	21.1	22.1	23.7	24.5	23.7	23.2	21.5	22.5
33.5	23.9	24.5	24.4	24.8	24.3	24.8	21.1	22.1	23.8	24.6	23.8	23.2	21.5	22.5
34.0	24.1	24.7	24.5	24.9	24.3	24.9	21.1	22.1	23.8	24.7	23.9	23.3	21.5	22.6
34.5	24.1	24.8	24.7	25.1	24.4	25.0	21.1	22.1	23.9	24.8	23.9	23.3	21.5	22.6
35.0	24.2	24.9	24.8	25.1	24.4	25.1	21.1	22.1	24.0	25.0	24.0	23.4	21.5	22.6
35.5	24.3	25.0	–	25.1	24.5	25.1	21.1	22.1	24.1	25.0	24.1	23.4	21.5	22.6
36.0	24.4	25.2	–	25.2	24.6	25.2	21.1	22.1	24.2	25.1	24.2	23.5	21.5	22.6
36.5	24.6	25.2	–	25.2	24.7	25.2	21.1	22.1	–	25.2	24.3	23.6	21.5	22.6
37.0	24.6	25.3	–	25.3	24.7	25.2	21.2	22.2	–	25.2	24.3	23.6	21.5	22.6
37.5	24.7	25.5	–	25.3	24.8	25.3	21.2	22.2	–	25.2	24.3	23.7	21.5	22.6
38.0	24.7	25.6	–	25.4	24.8	25.3	21.2	22.2	–	25.2	24.4	23.8	21.6	22.7
38.5	24.7	25.7	–	25.5	24.9	25.4	21.2	22.2	–	25.3	24.6	23.9	21.6	22.7
39.0	24.8	25.7	–	25.5	24.9	25.5	21.3	22.3	–	25.4	24.8	23.9	21.6	22.7
39.5	24.9	25.8	–	25.7	25.0	25.6	21.3	22.3	–	25.5	24.9	24.0	21.6	22.7
40.0	24.9	25.9	–	25.7	25.1	25.6	21.3	22.3	–	25.5	24.9	24.1	21.7	22.8
40.5	–	25.9	–	–	25.1	25.6	21.4	22.4	–	–	–	24.2	21.7	22.8
41.0	–	25.9	–	–	25.2	25.7	21.4	22.4	–	–	–	24.3	21.7	22.8
41.5	–	25.9	–	–	25.2	25.7	21.5	22.4	–	–	–	24.4	21.8	22.8
42.0	–	26.0	–	–	25.3	25.8	21.5	22.5	–	–	–	24.5	21.8	22.9
42.5	–	26.0	–	–	25.4	25.9	21.6	22.5	–	–	–	24.6	21.8	22.9
43.0	–	–	–	–	25.4	25.9	21.6	22.6	–	–	–	24.7	21.8	22.9
43.5	–	–	–	–	25.5	26.0	21.7	22.6	–	–	–	24.7	21.9	23.0
44.0	–	–	–	–	25.5	26.0	21.7	22.7	–	–	–	24.8	21.9	23.0
44.5	–	–	–	–	25.6	26.0	21.7	22.7	–	–	–	24.9	21.9	23.0
45.0	–	–	–	–	25.6	26.1	21.8	22.8	–	–	–	25.0	21.9	23.0
45.5	–	–	–	–	25.7	–	21.8	22.8	–	–	–	25.1	22.0	23.1
46.0	–	–	–	–	25.7	–	21.9	22.9	–	–	–	25.2	22.0	23.1
46.5	–	–	–	–	25.7	–	21.9	22.9	–	–	–	25.3	22.1	23.1
47.0	–	–	–	–	25.8	–	22.0	23.0	–	–	–	25.4	22.1	23.1
47.5	–	–	–	–	25.9	–	22.0	23.0	–	–	–	25.5	22.1	23.2
48.0	–	–	–	–	25.9	–	22.1	23.0	–	–	–	25.6	22.2	23.2
48.5	–	–	–	–	25.9	–	22.1	23.1	–	–	–	25.7	22.2	23.3
49.0	–	–	–	–	26.0	–	22.2	23.2	–	–	–	25.7	22.3	23.3
49.5	–	–	–	–	26.0	–	22.3	23.2	–	–	–	25.8	22.4	23.3
50.0	–	–	–	–	26.0	–	22.3	23.3	–	–	–	25.9	22.4	23.4
50.5	–	–	–	–	–	–	22.4	23.4	–	–	–	–	22.4	23.4
51.0	–	–	–	–	–	–	22.5	23.4	–	–	–	–	22.5	23.5
51.5	–	–	–	–	–	–	22.6	23.5	–	–	–	–	22.5	23.5
52.0	–	–	–	–	–	–	22.6	23.6	–	–	–	–	22.5	23.5
52.5	–	–	–	–	–	–	22.7	23.7	–	–	–	–	22.6	23.6
53.0	–	–	–	–	–	–	22.8	23.7	–	–	–	–	22.7	23.6
53.5	–	–	–	–	–	–	22.8	23.9	–	–	–	–	22.7	23.7
54.0	–	–	–	–	–	–	22.9	23.9	–	–	–	–	22.7	23.7
54.5	–	–	–	–	–	–	23.0	24.0	–	–	–	–	22.8	23.7
55.0	–	–	–	–	–	–	23.1	24.1	–	–	–	–	22.8	23.7
55.5	–	–	–	–	–	–	23.2	24.2	–	–	–	–	22.8	23.8
56.0	–	–	–	–	–	–	23.2	24.3	–	–	–	–	22.9	23.8
56.5	–	–	–	–	–	–	23.3	24.3	–	–	–	–	–	–
57.0	–	–	–	–	–	–	23.4	24.4	–	–	–	–	–	–
57.5	–	–	–	–	–	–	23.5	24.5	–	–	–	–	–	–
58.0	–	–	–	–	–	–	23.6	24.5	–	–	–	–	–	–
58.5	–	–	–	–	–	–	23.6	24.6	–	–	–	–	–	–
59.0	–	–	–	–	–	–	23.6	24.7	–	–	–	–	–	–

Table 4: *Results of surface brightness profiles' decomposition into components*

Object (1)	Band (2)	PA (3)	b/a (4)	m_n (5)	r_n (6)	m_e (7)	r_e (8)	m_0 (9)	r_0 (10)
Mrk 3	I	56.0	0.94	17.31:	0.99	18.54:	3.91	19.30:	6.60
Mrk 3	V	56.0	0.94	18.32	1.33	19.27	3.88	21.00	10.88
Mrk 530	I	161.1	0.60	16.15	1.37	18.16	3.37	18.84	9.48
Mrk 530	V	161.1	0.60	16.83	1.28	18.90	2.95	20.09	11.38
Mrk 533	R	101.1	0.90	18.47	0.91	18.38	1.32	19.30	6.98
Mrk 533	V	101.1	0.90	17.97	0.90	18.93	1.42	19.99	8.79
Mrk 573	I	91.8	0.91	16.44	1.62	18.82	5.57	22.46:	25.71:
Mrk 573	V	91.8	0.91	17.49	1.69	20.06	5.28	21.88	13.04
Mrk 744	R	62.9	0.51	17.62	2.31	19.40	5.30	20.45	22.15
Mrk 744	V	62.9	0.51	18.37	2.42	20.18	5.57	20.94	21.94
Mrk 955	I	157.0	0.91	17.57	1.94	19.19	3.98	21.95:	13.22:
Mrk 955	V	157.0	0.91	18.46	1.74	20.34	3.58	22.57	13.18
Mrk 1058	I	113.8	0.57	18.37	1.41	18.43	2.22	18.48	5.41
Mrk 1058	V	113.8	0.57	19.24	1.49	20.12	2.58	20.06	6.02
Mrk 1066	I	129.0	0.67	16.71	2.27	18.74	5.61	21.27	17.21
Mrk 1066	V	129.0	0.67	18.08	2.14	20.11	5.46	22.21	17.00
Mrk 1073	I	91.9	0.70	17.15	1.45	19.62	4.82	18.66	6.80
Mrk 1073	V	91.9	0.70	18.21	1.28	20.79	4.22	19.84	7.26
Mrk 1157	I	178.0	0.96	17.46	1.06	18.53	2.19	18.46	6.04
Mrk 1157	V	178.0	0.96	18.32	1.04	19.78	2.08	19.69	7.04
NGC 1019	R	39.0	0.65	19.02	1.91	21.17	3.94	20.98	10.65
NGC 1019	V	39.0	0.65	19.86	2.07	21.95	4.23	21.65	11.05
NGC 3185	I	130.2	0.56	17.26	2.30	19.54	5.56	19.27	14.16
NGC 3185	V	130.2	0.56	18.45	2.18	20.86	5.36	20.36	13.80
UGC 524	I	129.7	0.95	16.97	1.41	19.45	4.08	20.91	12.34
UGC 524	V	129.7	0.95	18.25	1.44	20.70	4.07	21.76	11.83
UGC 3223	V	77.0	0.55	19.64	1.58	20.54	2.80	19.78	8.61
UGC 3995	I	95.0	0.55	17.23	2.95	19.65	8.61	19.58	18.19
UGC 3995	V	95.0	0.55	18.73	3.39	21.12	10.23	20.94	20.63

Notes: (1) - the object name; (2) - range; (3,4) - parameters of ellipses for the profile construction; (5,6) - parameters of the nucleus; (7,8) - parameters of the bulge; (9,10)- parameters of the disk; PA - in degrees; m_n, m_e, m_0 - in $^m/\square''$; r_n, r_e, r_0 - in arcseconds; (:).- uncertain values.

distance ($m_e = m_b(r_e)$).

For approximation of the profile of the central star-like nucleus we used a Gauss function in the form:

$$m_n(r) = m_0 + 0.753 r^2/w^2, \qquad (5)$$

where m_0 is the surface brightness at the centre, w is the half-width at half maximum intensity. The latter is determined by the image quality.

At the first stage the decomposition of the profiles into the components was performed by selection of parameters of the components in an interactive mode. The disk, bulge and the central nucleus brightness distributions were modelled by equations (1), (2) and (5), respectively. The results of decomposition are given in Fig. 2 b. The great excesses in the central regions of the galaxies are caused by the presence of bars and ring-like structures. The outer parts are accordingly distorted by spiral arms and outer rings.

At the next stage the components were decom-

posed by the non-linear least squares method. To diminish the influence of spiral arms and rings in the outer regions of the disk, an addition Gauss function was introduced formally:

$$m(r) = m_0 e^{-(r-r_c)^2/r_0{}^2}, \qquad (6)$$

where r_c is the position of the maximum on the profile, m_0 is the additive correction at a distance r_c, r_0 is the scale parameter. The brightness distributions of the disk and nucleus were approximated by exponential law (1) and Gaussian (5). The brightness distribution of the bulge at the first stage was simulated by Vaucouleurs law (2), however, in this case its parameters would often turn out physically unfit. This might be due to the small size of the bulge. Besides, nearly all programme objects possess either bars or rings, which may essentially distort the profile in the central regions of the galaxies.

The situation improved considerably when approximating the brightness distribution of the bulge

by generalized exponential law (4) with $n = 0.5$. That is why, except for Mrk 3, all the profiles were decomposed into the components, using the brightness distribution of the bulge represented by (4). Only in the case of Mrk 3 satisfactory results were obtained applying the Vaucouleurs law for bulge.

5. Results

The results of decomposition of the profile components by the numerical non–linear least squares method are displayed in Fig. 2 a.

Here in most of the objects the distribution of the bulge brightness was modelled by the Gauss function (4), and only in one galaxy (Mrk 3) the modelling was done by the Vaucouleurs law (2).

In Fig. 2 b is shown the profile decomposition in the interactive mode with application of Vaucouleurs law (2) for modelling of brightness distribution of bulge.

It is seen from Fig. 2a that nearly in all the objects the differences between the observed and model brightness profiles turned out small (the residuals are presented at the bottom of Fig. 2a, b in stellar magnitudes). With the interactive decomposition (the bulge brightness distribution was represented by the Vaucouleurs law) the residuals were large (Fig. 2b) due to the presence of bright bars.

Thus, in the majority of the objects studied, the brightness distribution of the spherical component is impossible to represent satisfactorily by the Vaucouleurs law. Apparently, the bars, whose distribution of brightness can be described by a generalized exponential law, are the main contributor to the radiation of the spherical component of these objects.

The photometric parameters of the different components obtained from the decomposition of the brightness profiles by the numerical non–linear least–square method are listed in Table 4, where the unreliable values are marked by the colon. The disk parameters of the galaxies Mrk 573 and Mrk 955 in the I band have been determined with uncertainty because of the obvious underexposure of the outer parts of these galaxies (see Section 3 in Afanasiev et al., 1998). For the same reason I image of UGC 3223 was not analysed. The surface brightness in the I band for the galaxy Mrk 3 may be shifted by $\approx 0.4^m$ because of a possible systematic error at zero–point (see Section 3).

Note that in order to determine the parameters of the components a two–dimensional method has to be used, that is analyze the image, but not the brightness profiles. In the paper by de Jong (1996) the decomposition into components of CCD images of 86 normal spiral galaxies with well–distinguished disks $(b/a > 0.5)$ was accomplished using both the one–dimensional and the two–dimensional techniques.

When the two–dimensional method was applied, the brightness distribution of the bulges (bars) was represented by a generalized exponential law. Comparison of the parameters of the components for both methods of decomposition shows them to be practically coincident for the disks but considerably different for the bulges. Therefore extreme care should be used in treating the parameters of bulges given in Table 4.

Nevertheless, the parameters we derived for the spherical component can be used to determine the total contribution (bar + bulge) to the radiation of the host galaxy. As previously stated, the Gaussian (a particular case of the generalized exponential law) can satisfactorily be applied to represent the sum component. In the case of disks the parameters turn out to be correct even with the one–dimensional decomposition into the components (de Jong, 1996), and they can be compared with those in normal galaxies. Consequently we are planning to apply the two–dimensional method to refine the parameters of the bulges, while the value derived here may be treated as a zero approximation.

Using the results of the profile decomposition into the components, which were obtained by the numerical non–linear least squares method, integral magnitudes of the nucleus (N), bulge (B) and disk (D) were calculated. As the upper limit of integration for the bulge and nucleus a value of 3σ was taken. The disk was integrated to the maximum radius derived from the profile.

Then the integral magnitude of the host galaxy $(G = B + D)$, the ratio of the nucleus luminosity to the total luminosity of the host galaxy (N/G) and the contribution of the bulge (disk) to the integral luminosity of the galaxy (B/G) were determined. The data obtained are given in Table 5.

The mean central surface brightness of the disks (in $^m/\square''$) computed from our data is 20.9 ± 1.0 in V and 19.6 ± 1.0 in I bands.

From our data the mean value of B/G makes 0.22 ± 0.18 and 0.21 ± 0.17 in the V and I bands, respectively. Hence it follows that the mean value of relative contribution of the disk component into the luminosity of the host galaxy is about 0.8, i.e. these are the objects with well pronounced disks.

6. Conclusion

In the present paper results are given of surface photometry of 15 Seyfert galaxies in the V and I(R) colour bands. CCD images of these objects were obtained with the 1 m Zeiss telescope of SAO RAS. The limiting measurable surface brightness (at the level $S/N \approx 5$) was $(25.0–25.5)^m/\square''$ in V and R bands and $(24.0–24.5)^m/\square''$ in I band.

A comparison made shows our photometrical results to be in good agreement with the data of other

Table 5: *The integral luminosity of the host galaxies (G), the ratio of the nucleus luminosity (N/G) and of the bulge (B/G) to the integral luminosity of the host galaxy.*

Object	Band	G	N/G	B/G
Mrk 530	V	13.22	0.16	0.17
Mrk 533	V	13.38	0.05	0.07
Mrk 573	V	13.85	0.41	0.52
Mrk 744	V	13.17	0.11	0.15
Mrk 955	V	14.62	0.55	0.47
Mrk 1058	V	14.64	0.08	0.15
Mrk 1066	V	13.84	0.38	0.60
Mrk 1073	V	13.80	0.09	0.12
Mrk 1157	V	13.46	0.05	0.08
NGC 1019	V	14.88	0.13	0.11
NGC 3185	V	13.25	0.10	0.09
UGC 524	V	14.29	0.23	0.27
UGC 3223	V	13.72	0.03	0.05
UGC 3995	V	13.07	0.15	0.21
Mrk 530	I	12.33	0.15	0.20
Mrk 533	R	13.14	0.02	0.08
Mrk 744	R	12.65	0.12	0.18
Mrk 1058	I	13.28	0.05	0.15
Mrk 1066	I	12.66	0.50	0.68
Mrk 1073	I	12.70	0.11	0.17
Mrk 1157	I	12.50	0.05	0.11
NGC 1019	R	14.25	0.13	0.11
NGC 3185	I	12.08	0.11	0.11
UGC 524	I	13.31	0.29	0.34
UGC 3995	I	11.91	0.16	0.20

authors (the differences are within 0.1^m).

Surface brightness profiles azimuthally averaged in elliptical rings have been constructed. In the frame of a three–component model of the galaxy (nucleus, bulge, disk), decomposition of the brightness profiles into components have been performed in two ways: by the numerical non–linear least squares method and by the interactive technique. In so doing the brightness distribution of the nucleus and that of the disk were represented by the Gaussian and by the exponential law, respectively. Two functions were used to simulate the brightness distribution in the bulge: the generalized exponential law and the Vaucouleurs law. Satisfactory agreement between the observed and model profiles have been found: a) for 14 objects in the case when the bulge brightness distribution is described by the Gaussian, as a specific case of the generalized exponential law; b) for one object (Mrk 3) if the brightness distribution of the bulge follows the Vaucouleurs law.

From the results of numerical decomposition of the brightness profiles into the components the parameters of the spherical and disk subsystems have been found. By integrating the model functions with these parameters, we have obtained: the integral stellar magnitudes of the host galaxies as a sum of luminosities of the bulge and disk (without Seyfert nucleus); the contribution of the bulge (disk) to the luminosity of the host galaxy; the ratio of the luminosity of the star–like nucleus to the integral luminosity of the host galaxy. All the objects studied are spiral galaxies (see Table 1) slightly inclined to the line of sight (b/a>0.5 according to Table 4) and therefore having, most likely, a minor proper absorption. Most of the galaxies have well–distinguished disks whose contribution to the luminosity of the host galaxy is about 80 %.

References

Adams T.F., 1977, Astrophys. J. Suppl. Ser., **33**, 19

Afanasiev V.L., 1981, Pis'ma Astron. Zh., **7**, 390

Afanasiev V.L., Doroshenko V.T., Terebizh V.Yu., 1986, Astrofizika, **24**, 333

Afanasiev V.L., 1987, in: Martynov D.Ya., (ed.) "Active nuclei and stellar cosmogony (in Russian), Publ. MSU, 34

Afanasiev V.L., Dodonov S.N., Borisenko A.N., Markelov S.V., Ryadchenko V.P., 1991, Prepr. SAO, No. **76**

Afanasiev V.L., Mikhailov V.P., Shapovalova A.I., 1998, Astron. Astrophys. Trans., **17** (in press)

Caon N., Capacioli M., D'Onofrio M., 1993, Mon. Not. R. Astron. Soc., **265**, 1013

Christian C.A., Adams M., Barnes J.V., Butcher H., Hayes D.S., Mould J.R., Siegel M., 1985, Publ. Astr. Soc. Pacific, **97**, 363

Cousins A.W.J., 1976, Mem.R.A.S., **81**, 25

De Jong R.S., van der Kruit P.C., 1994, Astron. Astrophys. Suppl. Ser., **106**, 451

De Jong R.S.,1996, Astron. Astrophys. Suppl. Ser., **118**, 557

De Vaucouleurs G., 1948, Ann. d'Astrophys., **11**, 247

De Vaucouleurs A., Longo G., 1988, The University of Texas Monographs in Astronomy, No. **5**

Doroshenko V.T., Terebizh V.Yu., 1979, Pis'ma Astron. Zh., **5**, 571

Doroshenko V.T., Terebizh V.Yu., 1981, Astrofizika, **17**, 667

D'Onofrio M., Capaccioli M., Caon N., 1994, Mon. Not. R. Astron. Soc., **271**, 523

Granato G.L., Zitelli V., Bonoli F., Danese L., Bonoli C., Delpino F., 1993, Astrophys. J. Suppl. Ser., **89**, 35

Hubble E.P., 1930, Astrophys. J., **71**, 231

King I.R., 1966, Astron. J., **71**, 64

Kotilainen J.K., Ward M.J., Williger G.M., 1993, Prep. ESO, No. **908**

Landolt A.U.: 1992, Astron. J., **104**, 340

Lipovetsky V.A., Neizvestny S.I., Neizvestnaya O.M., 1987, Soobshch. SAO, **55**, 1

MacKenty J.W., 1990, Astrophys. J. Suppl. Ser., **72**, 231

Márquez I., 1996, in: Buta R., Crocke D.A. and Elmegreen B.G. (eds), IAU Colloq. 157, "Barred Galaxies", ASP Conf. Ser., **91**, 21

McLeod K.K. & Rieke G.H., 1994, Astrophys. J., **420**, 58

Mediavilla E., Pastoriza M.G., Bateher E., 1989, Astrophys. Space Sci., **157**, 145

Mikhailov V.P., 1986, Soobshch. SAO, **50**, 71

Mulchaey J.S., Regan M.W., Kundu A., 1997, Astrophys. J. Suppl. Ser., **110**, 299

Moles M., Márquez I., Pérez E., 1995, Astrophys. J., **438**, 604

Neizvestny S.I., 1988, "Investigation of photometric distinctions of Seyfert galaxies", Thesis, Nizhnij Arkhyz

Nelson C.H. & Whittle M., 1995, Astrophys. J. Suppl. Ser., **99**, 67

Nelson C.H. & Whittle M., 1996, Astrophys. J., **465**, 96

Seyfert K., 1943, Astrophys. J., **97**, 28

Simkin S.M., Su H.J., Schwarz M.P., 1980, Astrophys. J., **237**, 404

Su H.J., Simkin S.M., 1980, Astrophys. J., **238**, L1

Whittle M., 1992a, Astrophys. J. Suppl. Ser., **79**, 49

Whittle M., 1992b, Astrophys. J., **387**, 109

Whittle M., 1992c, Astrophys. J., **387**, 121

Wozniak H., Friedli D., Martinet L., Martin P., Bratschi P., 1995, Astron. Astrophys. Suppl. Ser., **11**, 115

Yee H.K., 1983, Astrophys. J., **272**, 473

Zasov A.V., Lyuty V.M., 1973, Astron. J., **50**, 253, 1981, Pis'ma Astron. Zh., **7**, 459

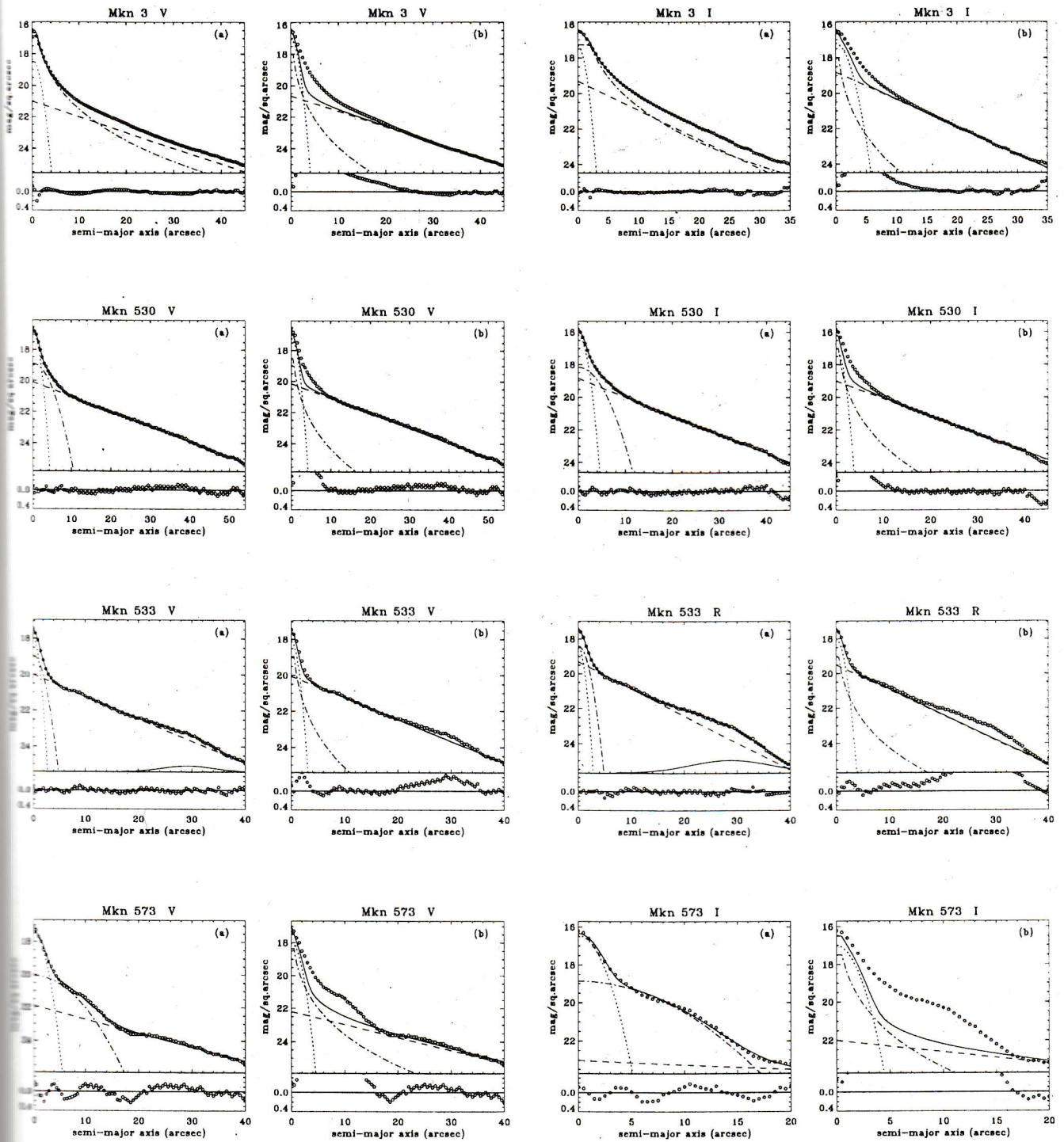Zasov A.V., Neizvestny S.I., 1989, Pis'ma Astron. Zh., **15**, 963

Fig. 2: *The results of separation of the surface brightness profiles into components: a) by the numerical non-linear least-squares method, b) by selection of the parameters in the interactive mode. The circles in the upper part of the diagram denote the original surface brightness profiles, the dotted line is the star-like nucleus profile, the dash-and-dot line is the bulge profile, the dashed line is the disk profile, the solid line is the total model profile with allowance for the distortion caused by the spiral structure and the rings. On the abscissa the semi-major axis of the ellipse in arcseconds is plotted. The surface brightness in stellar magnitudes per square arcseconds is laid off as ordinate. In the lower part of the diagram the circles show the difference between the observational profile and model one.*
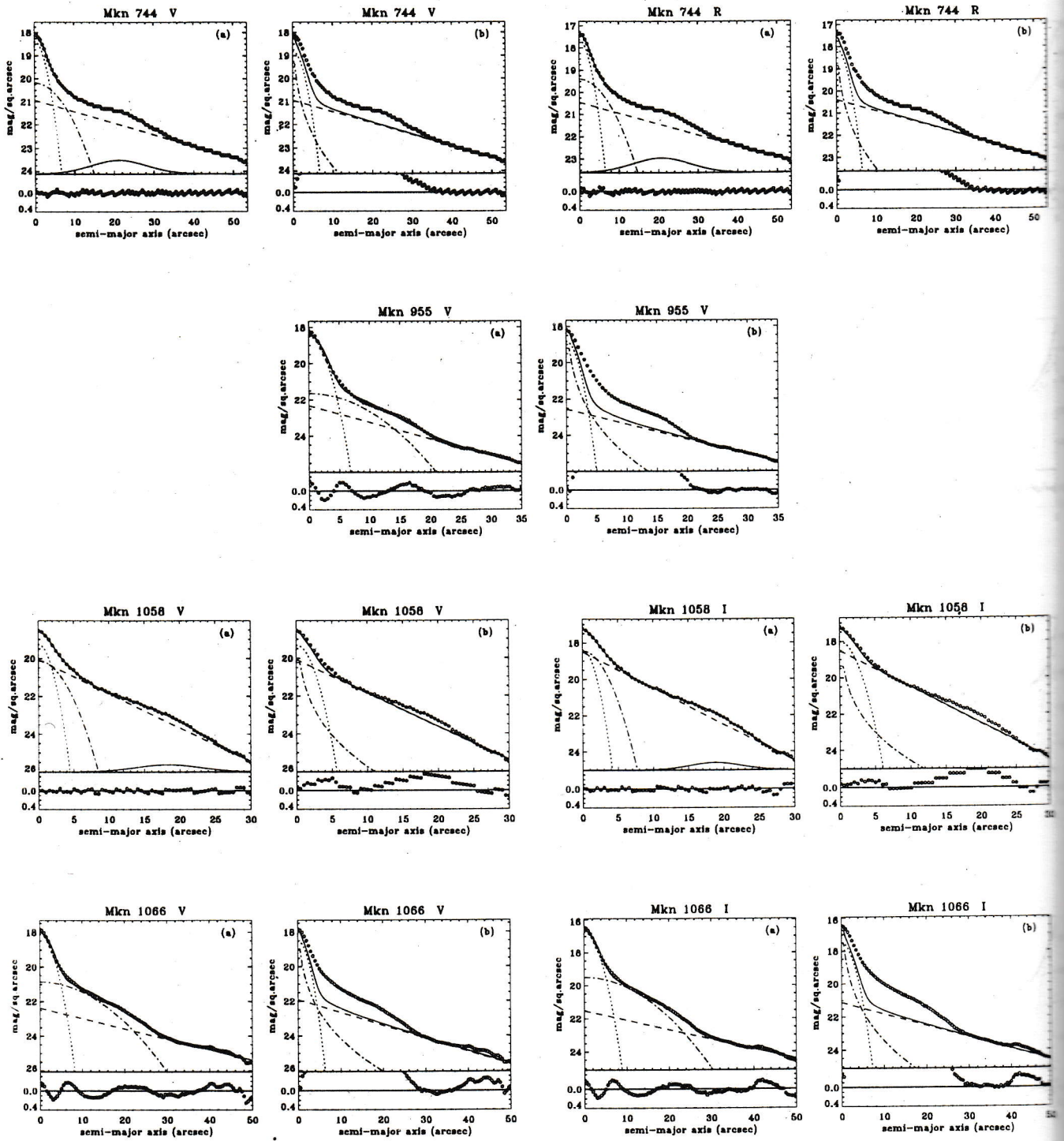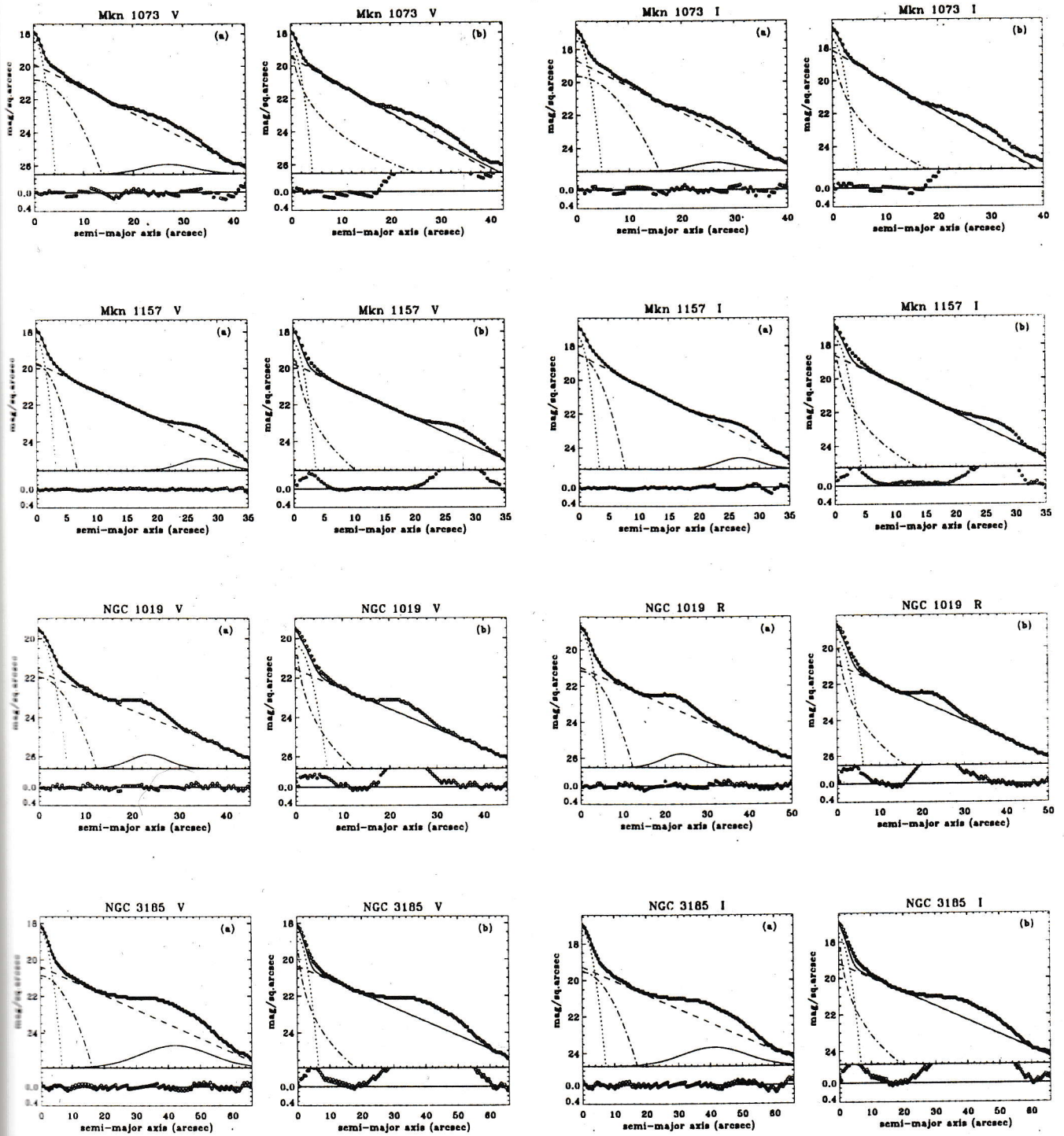
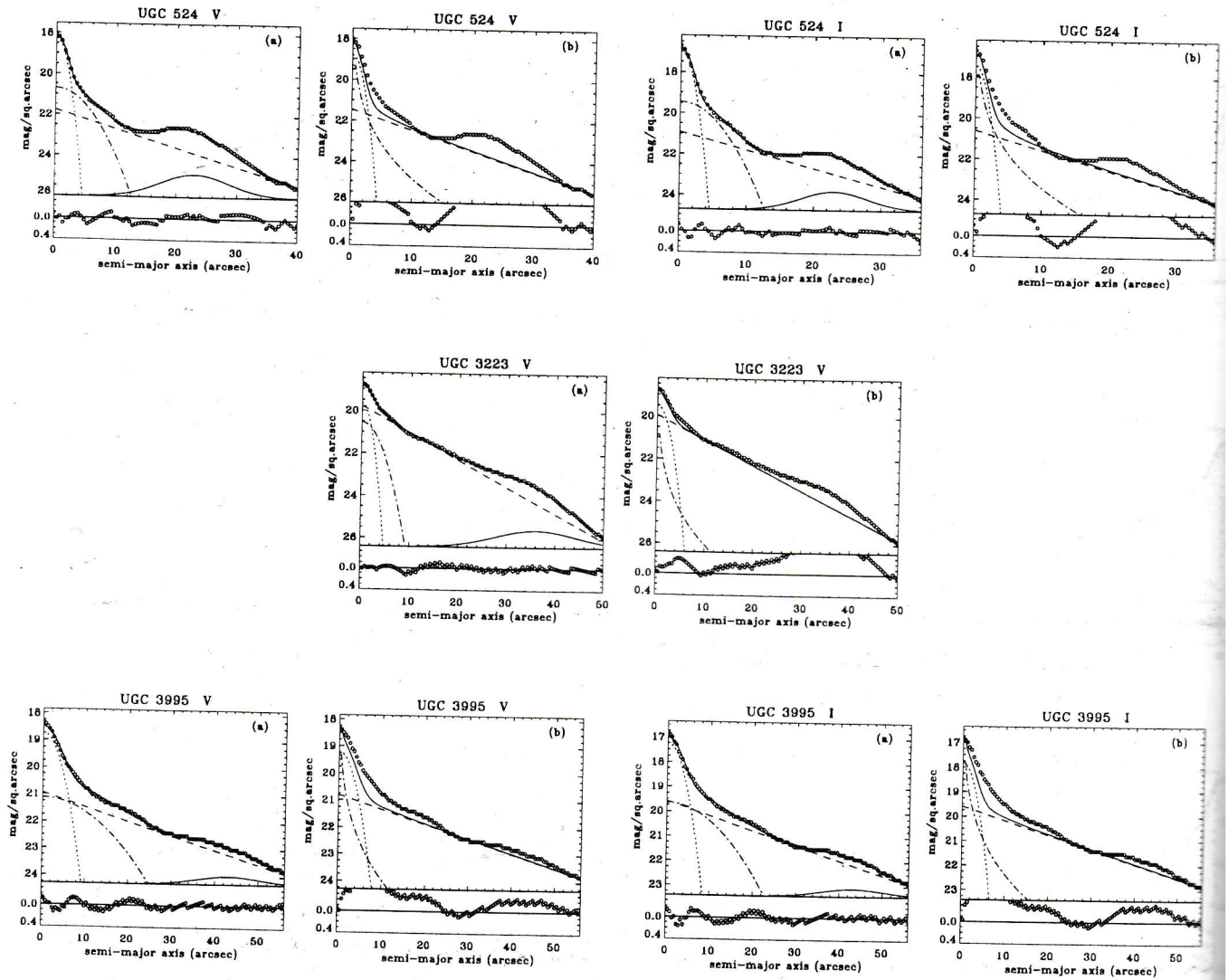Fig. 2: *(continued)*

Fig. 2: *(continued)*

Fig. 2: *(continued)*